Research Article GU J Sci, Part A, 10(1): 9-19 (2023) 10.54287/gujsa.1206972

Gazi University
Journal of Science
PART A: ENGINEERING AND INNOVATION
http://dergipark.org.tr/gujsa

The Comparison of the Temperature Susceptibility of the Serial Resistance Effect of Au/n-GaAs Type M/S Structures

Esra EVCİN BAYDİLLİ[1*]

[1]*Hakkari University, Faculty of Engineering, Department of Electrical and Electronics Engineering, Hakkari, Türkiye*

Keywords

M/S Structures
Serial Resistance
Ohm's Law
Cheung-Cheung Functions
Norde Function

Abstract

To enable comparison with the literature, this study seeks to assess the temperature susceptibility of serial resistance (Rs) features of the Au/n-GaAs type M/S structure, which is acceptable the benchmark sample. The serial resistance features of the sample were computed separately withal principal of Ohm, Norde, and Cheungs' functions. The current-voltage (I-V) data used in order to compute were evaluated at the voltage values between +2V and -2 V and temperature values between 120K and 360K in 60K steps. Each computation method was also compared one another other. As a result, the fact that the R_s values computed using principal of Ohm, Norde functions and Cheungs' functions tended to reduce with rising temperature, as anticipated by the literature results. In addition, it was determined that, with only tiny variations, the temperature susceptibility of R_s is consistent across all computation methods. In addition, as a result of the comparison with the literature, it was concluded serial resistance is less of an issue when a polymer interfacial layer is present at the metal-semiconductor contact region. The R_s parameter of the M/S structure is, in essence, a sensitive function of temperature and input voltage.

Cite

Evcin Baydilli, E. (2023). The Comparison of the Temperature Susceptibility of the Serial Resistance Effect of Au/n-GaAs Type M/S Contacts. GU J Sci, Part A, *10*(1), 9-19.

Author ID (ORCID Number)

E. Evcin Baydilli, 0000-0001-8582-5041

Article Process

Submission Date	18.11.2022
Revision Date	22.11.2022
Accepted Date	29.11.2022
Published Date	21.02.2023

1. INTRODUCTION

Metal/semiconductor (M/S) structures are extensive on the developing the microelectronics industry (Özdemir et al., 2021). Previously, silicon was widely used as a semiconductor in M/S structures, obtained by tight metal contact with a semiconductor. After that, GaAs became competitive with silicon due to its high electron mobility and increasing demand for devices operating at microwave frequency (Novoselov et al., 2004; Sadao, 2005). Its wide band gap of 1.42 eV makes GaAs a more resistant material against radiation. These features make it suitable for communication, aviation and space systems. In addition, GaAs, a direct band gap semiconductor, is ideal for optoelectronic devices (Çiçek et al., 2016). Au/n-GaAs is a fundamental and well-known type of M/S structures (Helal et al., 2020). Then, since the junction region properties of M/S structures significantly affect the contact performance, an interface layer has started to be placed between the M/S to control the charge transitions, prevent diffusion and leakage currents, and passivate the interface states (Sato and Yasumura, 1985; Altındal Yerişkin, 2019). In this study, the Au/n-GaAs type sample was accepted as a reference sample to compare the serial resistance properties of the M/S structures with an interfacial layer such as MIS and MPS types structures.

In M/S structures, the image-force, the tunneling, the edge, and the serial resistance effects are the factors that cause deviation from the ideal condition (Evcin Baydilli et al., 2020). The serial resistance (R_s) effect, among the most crucial of them, is the semiconductor's neutral region's resistance to the flow of current across the M/S contact, which is located outside the deplation region. (Deniz et al., 2022). As the positive voltage values increase, the R_s effect starts effective and the contact current declines as a result. (Ashajyothi & Reddy, 2021).

*Corresponding Author, e-mail: esraevcin@hakkari.edu.tr

The cause of this reduction in current is that when the voltage applied to the contact increases, the saturation effect occurs with the serial resistance effect and reduces the contact current (Rhoderick, 1978). So, this causes serious computation errors originating from R_s (Evcin Baydilli et al., 2020). Features such as conductor wire taken from M/S structures for measurements, the affinity of ohmic contact with semiconductor crystal, a dirty film layer formed on the interface, the semiconductor in the M/S structures has a disordered contribution distribution, the resistance of the M/S contact's depletion region on the semiconductor side, and the ohmic contact resistance causes a serial resistance effect (Sevgili et al., 2022).

This study focuses on the serial resistance effect of the Au/n-GaAs sample depending on temperature and voltage using principal of Ohm, Norde, and Cheungs' functions. Additionally, the outcomes of every method were contrasted with one another. The first method is principle of Ohm, the most well-known resistance computation method. The Norde method, developed by Norde, allows the calculation of R_s and potential barrier height (Φ_{Bo}) values using the F(V) function defined by a single I-V curve in which the temperature does not change when n=1 in its initial state (Norde, 1979). The Norde function was developed by Bohlin and allowed the computation of the R_s and Φ_{Bo} parameters of M/S structures if there is n>>1 (Bohlin, 1986). Another function that enables the analysis of R_s and other parameters (such as n, Φ_{Bo}) is the Cheungs' function. Cheungs' first function calculates the ideality factor (n) and R_s, and the second function, again, R_s and barrier height Φ_{Bo} were calculated. This method is considered a more straightforward method derived from I-V datas. In this approach, when the forward bias I-V curve precisely turns, R_s becomes active. (Cheung & Cheung, 1986).

In this research, the Au/n-GaAs type M/S structure's I-V data were evaluated at the voltage values between +2V and -2 V and temperature values between 120K and 360K in 60K steps. Because temperature is one of the most critical factors affecting the M/S structures parameters (Çaldıran, 2020), it is necessary to analyze the temperature susceptibility. Moreover, the n, R_s, and Φ_{Bo} parameters were also computed one by one by principal of Ohm, Norde, and Cheungs'functions. Computing these parameters with different methods will allow us to obtain valid and reliable results for the sample, making it possible to compare the results with the literature.

2. MATERIALS AND METHODS/EXPERIMENTAL METHODS

The n-GaAs semiconductor in the Au/n-GaAs type M/S structure was acquired by the Molecular Beam Epitaxy (MBE) method. The thickness of the n-GaAs semiconductor substrate is about 1 µm, its radius is 3", and it has [1 0 0] surface orientation. First, chemical cleaning of n-GaAs was performed to clean the substrate's impurity. Therefore, the substrate was ultrasonically washed with acetone ((CH_3COH_3) and isopropyl alcohol (C_3H_8O), respectively. After the substrate was ultrasonically washed with 18 MΩ-cm de-ionized water, it was dried with nitrogen (N_2) gas for 3 minutes. After the chemical cleaning process, ohmic contacts were prepared using 99.999% pure gold (Au) metal on the matte face of the n-GaAs wafer utilizing the thermal evaporation system. The constructed ohmic contact measures around 150 nm thick. For the ohmic contact to have low resistance, the annealing process was executed in the nitrogen medium at 500 ^oC for 3 minutes. Then, Au rectifying contacts were prepared on the substrate's bright (front) surface withal the thermal evaporation method, by utilizing a mask that have 1mm diameter holes. The obtained rectifier contacts are approximately 150 nm thick and 1 mm in diameter. The prepared Au/n-GaAs type M/S structure is shown in Figure 1. Current-voltage (I-V) data of the sample were perused between 120K and 360K temperature values in 60K steps by Kheitley 2400 current voltage source and the measurements was performed in the vpf-475 cryostat. Temperature monitoring was done with the temperature control device, Lake Shore model 321. Figure 2 presents the measurement system.

3. RESULTS AND DISCUSSION

The Au/n-GaAs type M/S structure's I-V datas outcomes are displayed in Figure 3 for a temperature range of 120K to 360K with 60K steps. Around 1 V, the I-V curves' linearity starts to degrade, at which point the Rs effect can be seen for each temperature setting. The inset graph shows the linear region between 0.6 V and 0.95 V in the current-voltage curve. By the extrapolating of the area where the I-V graph is linear, it is passed from experimental to theoretical calculation. Using the results of these calculations and the equations given below, the results in Table 1 were obtained (Rhoderick, 1978);

$$I = I_o \exp\left(\frac{qV}{nkT}\right) \tag{1}$$

$$\ln(I) = \ln\left(I_o\right) + \frac{q}{nkT}V_D \tag{2}$$

$$\Phi_{Bo} = \frac{kT}{q}\ln\left(\frac{AA^*T^2}{I_o}\right) \tag{3}$$

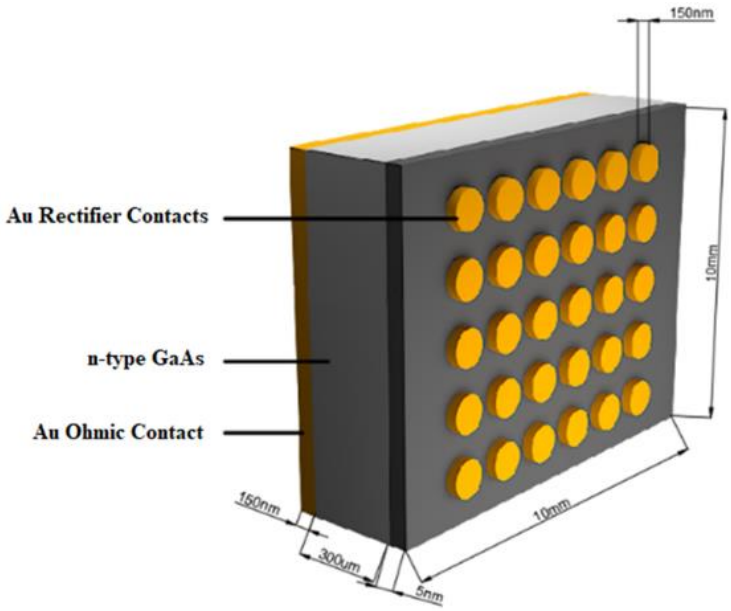

Figure 1. *The schematic presentation of the Au/n-GaAs type MS structure*

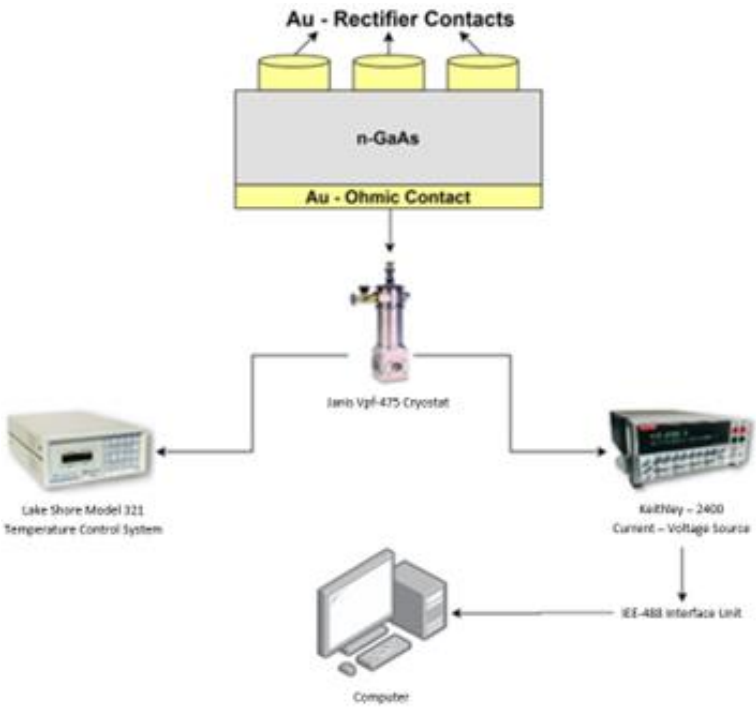

Figure 2. *The schematic presentation of the system for measuring.*

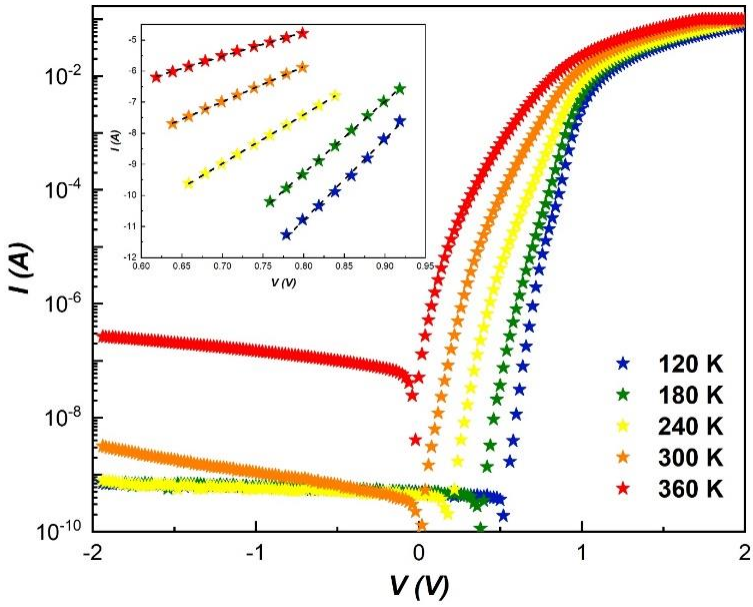

Figure 3. *The semilogarithmic I-V graph of Au/n-GaAs type M/S structure for each temperature value.*

Table 1. *n, Φ_{Bo}, and R_S parameters of Au/n-GaAs type M/S structure for each temperature value.*

T (K)	n	Φ_{Bo} (eV)	I_o (A)
120	2.25	0.398	8.13E-20
180	2.11	0.549	9.13E-15
240	1.44	0.582	5.95E-13
300	1.26	0.609	3.1E-10
360	1.04	0.622	6.94E-08

These findings suggest that the literature's description of barrier inhomogeneity as the cause of the decrease in n values and rise in Φ_{Bo} values with rising temperature (Werner & Güttler, 1991; Baydilli et al., 2020).

For each temperature setting, the graph of V vs. R_s is shown in Figure 4. Principle of Ohm was used to derive R_s values from forward bias values (Eq. 4) (Evcin Baydilli et al., 2020). As can be observed, temperature and applied voltage have a significant impact on the R_s values. Additionally, as Table 2's R_s values demonstrate, they drop as temperature rises. Because with increasing temperature, the carriers have more energy to overcome the barrier and higher voltage levels cause the I-V curve to bend, which indicates an increase in charge carrier density. (Taşyürek et al., 2022). So, the effect of R_s decreases. In the inset graph, it is seen that when the applied voltage increases, the values of R_s decrease. Recombination/generation CTMs (current-conduction mechanisms) can explain this phenomenon. (Werner and Güttler, 1991). In addition, after the temperature rises above room temperature, it is seen that the voltage-dependent R_s values converge as the temperature increases. This behavior can be explained by the Thermionic Emission theory becoming more effective after room temperature.

$$R_s = \frac{dV_i}{dI_i} \tag{4}$$

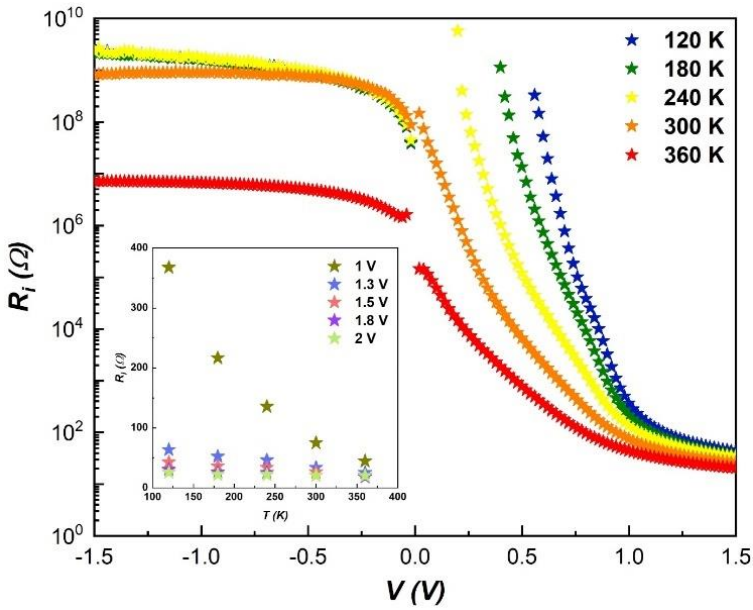

Figure 4. *R_i vs V_i and R_s vs T graph of Au/n-GaAs type M/S structure for each temperature value.*

Table 2. *R_S parameters of Au/n-GaAs type M/S structure for each temperature value.*

T (K)	R_s (Ω)
120	25.73
180	22.08
240	21.76
300	20.42
360	19.99

It has been stated that temperature and voltage have a considerable impact on the effect of R_s. The forward bias linear area changes as a result of this variability. That's why, it is helpful to refer to the Norde and Cheungs' functions to define the linear area of the positive voltage region. The graph of V vs. F(V), the outcome of the Norde function for each temperature value, is shown in Figure 5. The I-V features were utilized to derive the values of the ideality factors and current that are used in the F(V) function. The gamma (γ) value is a unitless integer created by adding to the n values by 2 (γ=n+2). Φ_{Bo} and R_s parameters were obtained by substituting V_{min} and I_{min} values to Eq. 5 and 6 (Uslu et al., 2010). The mentioned parameters and calculation results are shown in Table 3. It is seen that by increasing temperature values, R_s values decrease while Φ_{Bo} values increase.

$$F(V) = \frac{V}{\gamma} - \frac{kT}{q}\ln\left(\frac{I(V)}{AA^{*}T^{2}}\right) \tag{5}$$

$$R_s = \frac{(\gamma - n)kT}{qI_{\min}} \tag{6}$$

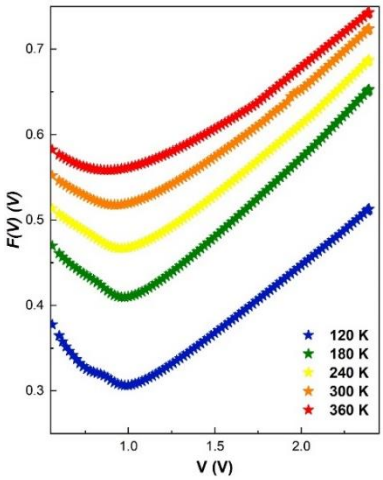

Figure 5. *F(V)-V graph of Au/n-GaAs type M/S structure for all temperatures.*

Table 3. *Some parameters obtained from the Norde function of Au/n-GaAs type M/S structure for each temperature value.*

T (K)	V_{min} (V)	$F(V)_{min}$ (V)	I_{min} (A)	Φ_{Bo} (eV)	R_s (Ω)	n	γ
120	0.98	0.306	0.0020	0.488	10.58	2.25	4.25
180	0.98	0.406	0.0036	0.622	8.54	2.11	4.11
240	0.94	0.488	0.0043	0.715	7.88	1.44	3.44
300	0.86	0.564	0.0050	0.794	6.36	1.26	3.26
360	0.72	0.621	0.0047	0.827	4.72	1.04	3.04

The graph in Figure 6a displays the linear results from Cheungs' first function, which are depicted in Eq.7 (Uslu et al., 2010). The n values were derived from the ordinate intersection point and the R_s values from the slope by fitting this linear region. Figure 6b shows the linear regions obtained from Cheung's second function, which is given in Eq. 8 (Uslu et al., 2010). The n value used in Cheung's second function is obtained from Cheungs' first function. From these linear regions' slopes, R_s values were computed, and from the ordinate intercept points, Φ_{Bo} values were computed. Table 4 shows the obtained results. The n values drop as the temperature values rise, while the Φ_{Bo} values rise. It is seen that the R_s values derived from the first and second Cheungs' functions are consistent with one another and reduce as the temperature value rises.

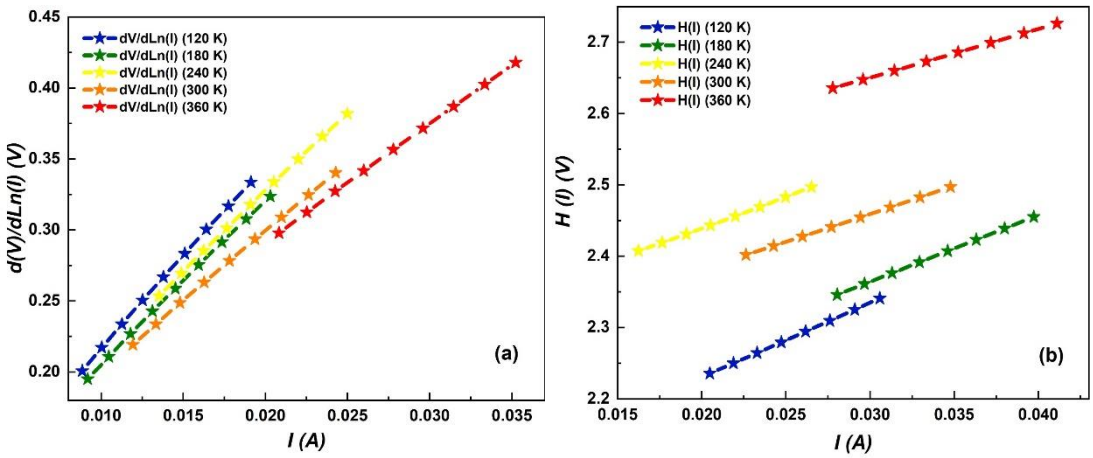

Figure 6. *The graph of **a)** Cheungs' first function **b)** Cheung's second function for Au/n-GaAs type M/S structure for each temperature value*

Table 4. *n, R_s, and Φ_{Bo} values obtained from Cheungs' functions of Au/n-GaAs type M/S structure for each temperature value*

	1st Function of Cheungs'		2nd Function of Cheungs'	
T (K)	**n**	**R_s (Ω)**	**R_s (Ω)**	**Φ_{Bo} (eV)**
120	8.45	12.932	10.428	0.239
180	5.79	11.581	9.342	0.360
240	4.97	11.213	8.714	0.456
300	3.98	9.801	7.838	0.558
360	4.03	8.321	6.809	0.607

Figure 7 shows temperature-dependent serial resistance computed by the principle of Ohm, Norde and Cheungs' first and second functions. With a few small variations brought on by the various I-V regions that each method considers, it can be argued that the behavior of the results acquired with each method are consistent with one another (Evcin Baydilli et al., 2020; Pehlivanoglu, 2021). The interface carriers are trapped, the concentration of free carriers diminishes, and the serial resistance effect grows as the n values rise with decreasing temperature (Evcin Baydilli et al., 2020).

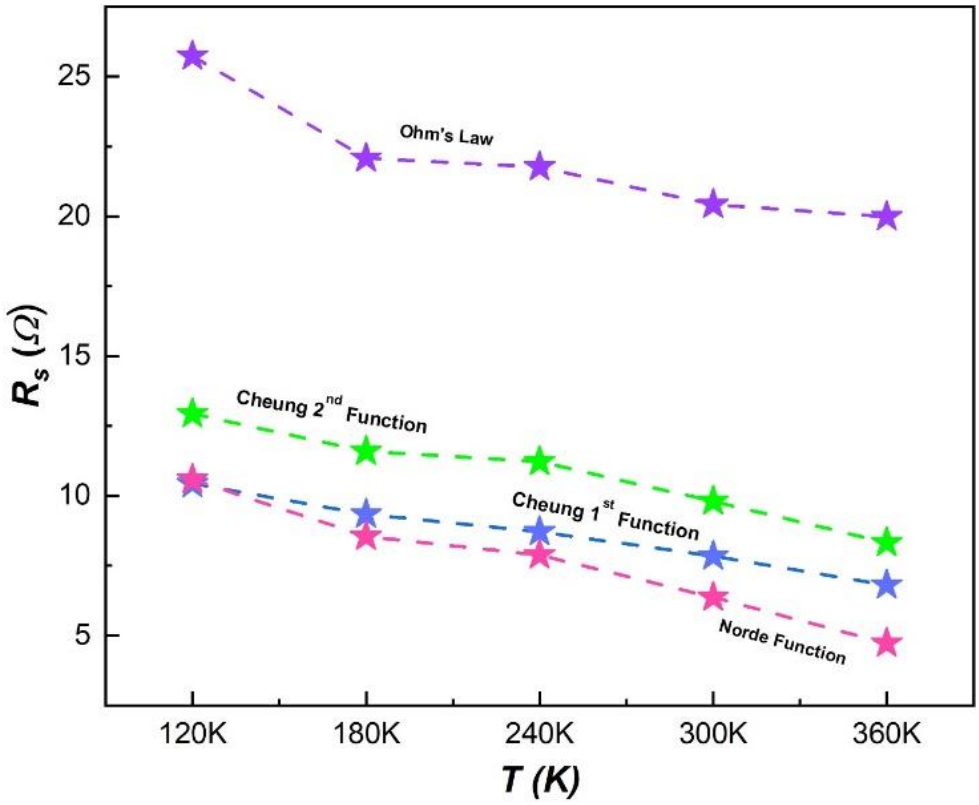

Figure 7. *Temperature-dependent R_s values of Au/n-GaAs type M/S structure according to Ohm's Law, Norde and Cheungs' Functions.*

Figure 8 belongs to our previous study (Evcin Baydilli et al., 2020). Unlike in Au/n-GaAs type M/S structure, there is a 7% Gr doped-PVA interfacial layer. In Figure 8, partial leaps are seen. This behavior can be explained by the fact that the different current-conduction mechanisms are active together or alone (Evcin Baydilli et al., 2020). On the other hand, it can be said that the effect of R_s decreases with increasing temperature for all

methods. In addition, it is seen that the serial resistance values of Au/(%7 Gr-doped)PVA/n-GaAs type M/P/S structure are lower than the serial resistance values of Au/n-GaAs type M/S structure. It could be asserted that the reason for these differences seen in Figure 7 and Figure 8 is the existence of the %7 Gr doped-PVA interfacial coating.

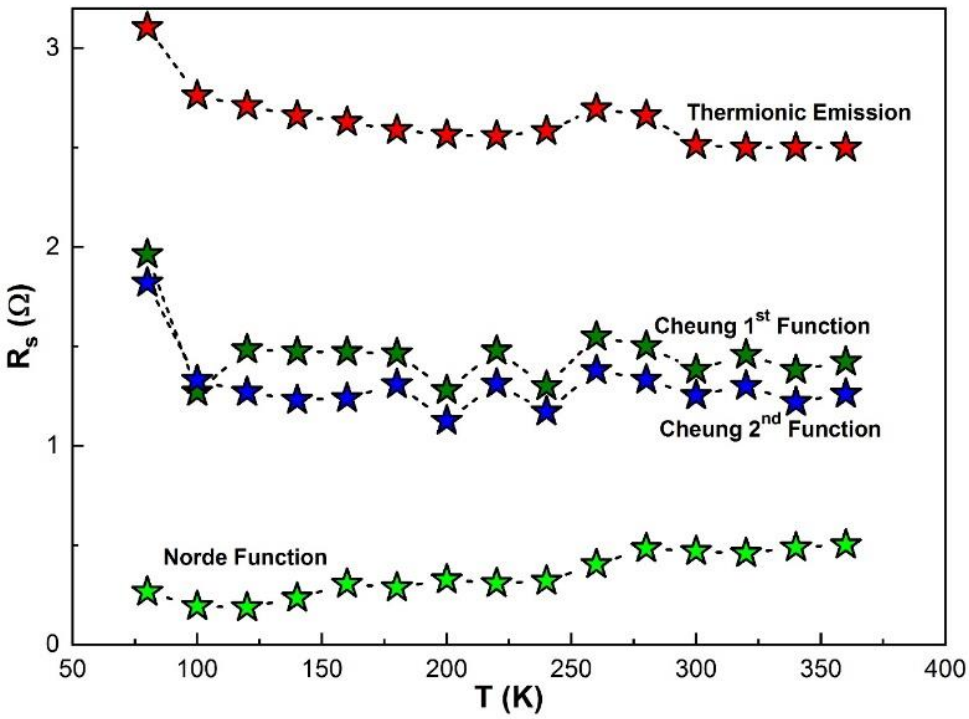

Figure 8. *Temperature-dependent R_s values of Au/(%7 Gr-doped)PVA/n-GaAs type M/P/S structure according to Principle of Ohm, Norde and Cheungs' Functions (Evcin Baydilli et al., 2020).*

Table 5 shows the comparison of the temperature-dependent changes of the n, R_s and Φ_{Bo} values obtained by principle of Ohm, Norde and Cheungs' functions of Au/n-GaAs type M/S and Au/(7% Gr-doped)PVA/n-GaAs type M/P/S structures. By the increase in temperature, the ideality factors of both structures decreased. When we compare the ideality factor values of the two structures, it is seen that the n values of the M/S structure are lower than those of the M/P/S structure. When the Φ_{Bo} values are examined, it is seen that the Φ_{Bo} values of both structures decrease with the increase in temperature. When the Φ_{Bo} values of the two structures are compared, it is seen that the Φ_{Bo} values of the M/P/S structure are lower than the Φ_{Bo} values of the M/S structure. It can be said that this difference between the two structures is due to the polymer interfacial layer. In addition, the temperature-dependent behavior of n and Φ_{Bo} values of both structures is explained by barrier inhomogeneity in the literature (Evcin Baydilli et al., 2020).

4. CONCLUSION

In this study, serial resistance properties of Au/n-GaAs type M/S structure depending on temperature and voltage, were investigated by three diverse methods: principle of Ohm, Norde, and Cheungs' functions. I-V measurements taken at ±2 V voltage and 120K-360K temperature range were used for computation process. The findings indicate that the Rs values, which are calculated by three methods, decreased with the increase in temperature. Additionally, with a few minor exceptions, the R_s values are likewise compatible with one another. That explains these slight variations caused by the various I-V regions that are considered by all methods. It has been found that the existence of the interface coating in M/S structures lessens the impact of serial resistance as compared to the literature. It is therefore determined that the serial resistance characteristics of Au/n-GaAs type M/S type structures are a decisive function of temperature and applied voltage.

Table 5. *Comparative representation of n, R_s, and Φ_{Bo} values obtained by Principle of Ohm, Norde and Chungs' functions of Au/n-GaAs type M/S and Au/(%7 Gr-doped)PVA/n-GaAs type MPS structures (Evcin Baydilli et al., 2020)*

Methode/Temperature	120 K	180 K	240 K	300 K	360 K
Ohm's Law (for Au/n-GaAs)					
R_s (Ω)	25.73	22.08	21.76	20.42	19.99
Φ_{Bo} (eV)	0.398	0.549	0.582	0.609	0.622
n	2.25	2.11	1.44	1.26	1.04
Ohm's Law (for Au/(%7 Gr-doped)PVA/n-GaAs)					
R_s (Ω)	2.71	2.59	2.58	2.51	2.5
Φ_{Bo} (eV)	0.19	0.3	0.43	0.55	0.64
n	12.44	7.79	5.18	3.83	3.21
Norde Function (for Au/n-GaAs)					
R_s (Ω)	10.58	8.54	7.88	6.36	4.72
Φ_{Bo} (eV)	0.488	0.622	0.715	0.794	0.827
Norde Function (for Au/(%7 Gr-doped)PVA/n-GaAs)					
R_s (Ω)	0.19	0.29	0.32	0.47	0.5
Φ_{Bo} (eV)	0.23	0.34	0.45	0.55	0.67
Cheung's 1st Function (for Au/n-GaAs)					
R_s (Ω)	12.932	11.581	11.213	9.801	8.321
n	8.45	5.79	4.97	3.98	4.03
Cheung's 1st Function (for Au/(%7 Gr-doped)PVA/n-GaAs)					
R_s (Ω)	1.48	1.47	1.49	1.38	1.42
n	10.68	6.84	5.29	4.65	3.19
Cheung's 2nd Function (for Au/n-GaAs)					
R_s (W)	10.428	9.342	8.714	7.838	6.809
Φ_{Bo} (eV)	0.239	0.36	0.456	0.558	0.607
Cheung's 2nd Function (for Au/(%7 Gr-doped)PVA/n-GaAs)					
R_s (W)	1.27	1.31	1.3	1.22	1.26
Φ_{Bo} (eV)	0.19	0.28	0.39	0.46	0.65

ACKNOWLEDGEMENT

Some parts of this study are presented at the 9th International Conference on Materials Science and Nanotechnology for Next Generation (MSNG-2022).

REFERENCES

Altındal Yerişkin, S. (2019). The investigation of effects of (Fe_2O_4-PVP) organic-layer, surface states, and serial resistance on the electrical characteristics and the sources of them. *Journal of Materials Science: Materials in Electronics*, *30*, 17032-17039. doi:10.1007/s10854-019-02045-x

Ashajyothi, S., & Reddy, V. R. (2021). Influence of tin oxide (SnO_2) interlayer on the electrical and reverse current conduction mechanism of Au/n-InP Schottky junction and its microstructural properties. *Thin Solid Films*, *740*, 139001. doi:10.1016/j.tsf.2021.139001

Baydilli, E. E., Tan, S. O., Tecimer, H. U., & Altındal, S. (2020). Detection of current transport mechanisms for graphene-doped-PVA interlayered metal/semiconductor structures. *Physica B Condens Matter*, *598*, 412457. doi:10.1016/j.physb.2020.412457

Bohlin, K. E. (1986). Generalized Norde plot including determination of the ideality factor. *Journal of Applied Physics*, *60*(3), 1223-1224. doi:10.1063/1.337372

Cheung, S. K., & Cheung, N. W. (1986). Extraction of Schottky diode parameters from forward current-voltage characteristics. *Applied Physics Letters*, *49*(2), 85-87. doi:10.1063/1.97359

Çaldıran, Z. (2020). Fabrication of Schottky barrier diodes with the lithium fluoride interface layer and electrical characterization in a wide temperature range. *Journal of Alloys and Compounds*, *816*, 152601. doi:10.1016/j.jallcom.2019.152601

Çiçek, O., Tecimer, H. U., Tan, S. O., Tecimer, H., Altındal, Ş., & Uslu, İ. (2016). Evaluation of electrical and photovoltaic behaviours as comparative of Au/n-GaAs (MS) diodes with and without pure and graphene (Gr)-doped polyvinyl alcohol (PVA) interfacial layer under dark and illuminated conditions. *Composites Part B: Engineering*, *98*, 260-268. doi:10.1016/j.compositesb.2016.05.042

Deniz, A. R., Taş, A. İ., Çaldıran, Z., İncekara, Ü., Biber, M., Aydoğan, Ş., & Türüt, A. (2022). Effects of PEDOT:PSS and crystal violet interface layers on current-voltage performance of Schottky barrier diodes as a function of temperature and variation of diode capacitance with frequency. *Current Applied Physics*, *39*, 173-182. doi:10.1016/j.cap.2022.03.017

Evcin Baydilli, E., Altındal, S., Tecimer, H., Kaymaz, A., & Uslu Tecimer, H. (2020). The determination of the temperature and voltage dependence of the main device parameters of Au/7%Gr-doped PVA/n-GaAs-type Schottky Diode (SD). *Journal of Materials Science: Materials in Electronics*, *31*, 17147-17157. doi:10.1007/s10854-020-03799-5

Helal, H., Benamara, Z., Arbia, M. B., Khettou, A., Rabehi, A., Kacha, A. H., & Amrani, M. (2020). A study of current-voltage and capacitance-voltage characteristics of Au/n-GaAs and Au/GaN/n-GaAs Schottky diodes in wide temperature range. *International Journal of Numerical Modelling: Electronic Networks, Devices and Fields*, *33*(4), e2714. doi:10.1002/jnm.2714

Norde, H. (1979). A modified forward I - V plot for Schottky diodes with high serial resistance. *Journal of Applied Physics*, *50*(7), 5052-5053. doi:10.1063/1.325607

Novoselov, K. S., Geim, A. K., Morozov, S. V., Jiang, D., Zhang, Y., Dubonos, S. V., Grigorieva, I. V., & Firsov, A. A. (2004). *Electric Field Effect in Atomically Thin Carbon Films*, *306*(5696), 666-669. doi:10.1126/science.1102896

Özdemir, A. F., Göksu, T., Yıldırım, N., Turut., A. (2021). Effects of measurement temperature and metal thickness on Schottky diode characteristics. *Physica B Condens Matter*, *616*, 413125. doi:10.1016/j.physb.2021.413125

Pehlivanoglu, S. A. (2021). Fabrication of p-Si/n-NiO:Zn photodiodes and current/capacitance-voltage characterizations. *Physica B Condens Matter*, *603*, 412482. doi:10.1016/j.physb.2020.412482

Rhoderick, E. H. (1978). *Metal-Semiconductor Contacts*. Clarendon Press Oxford.

Sadao, A. (2005). *Properties of Group-IV, III-V and II-VI Semiconductors*. Hoboken (USA) Wiley&Sons.

Sato, K., & Yasumura, Y. (1985). Study of forward I - V plot for Schottky diodes with high serial resistance. *Journal of Applied Physics*, *58*(9), 3655-3657. doi:10.1063/1.335750

Sevgili, Ö., Orak, İ., & Tiras, K. S. (2022). The examination of the electrical properties of Al/Mg_2Si/p-Si Schottky diodes with an ecofriendly interfacial layer depending on temperature and frequency. *Physica E: Low-dimensional Systems and Nanostructures*, *144*, 115380. doi:10.1016/j.physe.2022.115380

Taşyürek, L. B., Aydoğan, Ş., Sevim, M., & Çaldıran, Z. (2022). Analysis of the temperature dependent electrical parameters of the heterojunction obtained with Au nanoparticles decorated perovskite strontium titanate nanocubes. *Journal of Alloys and Compounds*, *914*, 165140. doi: 10.1016/j.jallcom.2022.165140

Uslu, H., Altındal, S., Aydemir, U., Dökme, I., & Afandiyeva, I. M. (2010). The interface states and serial resistance effects on the forward and reverse bias I-V, C-V and G/ω-V characteristics of Al-TiW-Pd 2Si/n-Si Schottky barrier diodes. *Journal of Alloys and Compounds*, *503*(1), 96-102. doi:10.1016/j.jallcom.2010.04.210

Werner, J. H., & Güttler, H. H. (1991). Barrier inhomogeneities at Schottky contacts. *Journal of Applied Physics*, *69*(3), 1522-1533. doi:10.1063/1.347243